JOURNAL OF MAGNETIC RESONANCE **124,** 474–478 (1997)
ARTICLE NO. MN961061

COMMUNICATIONS

A Phase-Cycling Algorithm for Reducing Sidebands in Adiabatic Decoupling

THOMAS E. SKINNER* AND M. ROBIN BENDALL†‡

*Physics Department, Wright State University, Dayton, Ohio 45435; and †Varian NMR Instruments Division, 3120 Hansen Way, P.O. Box 10800, Palo Alto, California 94304-1030

Received June 18, 1996; revised November 8, 1996

Adiabatic decoupling is as dependent on well-designed phase cycles for performance as any broadband method. For example, the dramatic performance gains of STUD (*1*) compared to DAP-16 (*2*) are a result, primarily, of the different phase cycles chosen for implementation of each scheme. Each method employs a sech/tanh (hyberbolic secant) inversion pulse (*3*). In this article, we describe a simple algorithm (*4*) for improving the performance of broadband-decoupling schemes. New phase cycles constructed with this technique can significantly reduce sidebands and increase decoupling efficiency, allowing either lower RF power to achieve a desired decoupled bandwidth or larger bandwidth for a given RF power level. Examples providing progressive improvement in decoupling performance are tabulated for comparison.

The M4P5 phase cycle introduced by Fujiwara and Nagayama (*5*) has become a *de facto* standard for adiabatic decoupling. It consists of the specific P5 inversion cycle [0°, 150°, 60°, 150°, 0°] from the general prescription

$$[0°,\ d,\ 2d + 120°,\ 3d + 60°,\ 4d + 120°] \qquad [1]$$

of Tycko and Pines (*6*), overlaid by MLEV-4 (*7*). Originally used in conjunction with frequency-switched composite inversion pulses (*5*), M4P5 was shown to provide an exceptional method for broadband decoupling due to enhanced off-resonance inversion provided by the P5 cycle. Although adiabatic pulses can also exhibit outstanding broadband inversion properties, they were noted to cause considerable sidebands (*5*). Adiabatic decoupling would typically violate the fast-cycling condition $T_c J \ll 1$, where T_c is the time to return the irradated spins to their initial orientation, since the length, T_p, of even a single adiabatic inversion pulse can be a sizable fraction of $1/J$. However, pulse length and RF field strength can be varied independently in adiabatic decoupling, in contrast to composite-pulse methods, where the length of the sequence is inversely proportional to the RF amplitude. The above fast-cycling condition then becomes a more ambiguous gauge for sideband performance, since sideband levels can actually be decreased by increasing T_p when RF levels are below a threshold determined by the desired decoupled bandwidth (*8*). Thus, there are mitigating factors, and sech/tanh decoupling implemented with the efficient M4P5 phase cycle was shown to provide performance for large bandwidths that significantly exceeds composite-pulse methods (*1, 8*). This phase cycle provides similar benefits for other adiabatic decoupling methods (*9, 10*) compared to implementations using alternative cycles (*11, 12*). Further improvements in decoupling performance can be found by considering the behavior of M4P5 in more detail.

The value $d = 150°$ used in M4P5 is based on a plausible assumption that maximizing the average inverted z magnetization over a desired frequency-offset range will optimize the performance of the phase cycle for decoupling (*5*). Decoupling methods are typically evaluated using a sample containing a single value for the coupling constant J_{CH}. Off-resonance performance is assessed by varying the decoupler offset. We find that both the intensity of the maximum sideband at a given decoupler offset and the average sideband intensity over a given offset range are sensitive to the value of d in adiabatic decoupling. If we consider the distribution of maximum sideband amplitudes as a function of decoupler offset, we also find that changing d changes the particular offset at which the maximum of the distribution occurs. Yet, in hyperbolic secant decoupling, for example, the maximum in the sideband distribution over an effective decoupled bandwidth equal to ~90% of the adiabatic frequency sweep is relatively insensitive to the value of d. The strategy employed here is therefore to choose two different values of d

‡ Present address: Department of Chemistry and Chemical Engineering, School of Molecular Sciences, James Cook University of North Queensland, Townsville, 4811 Queensland, Australia.

1090-7807/97 $25.00

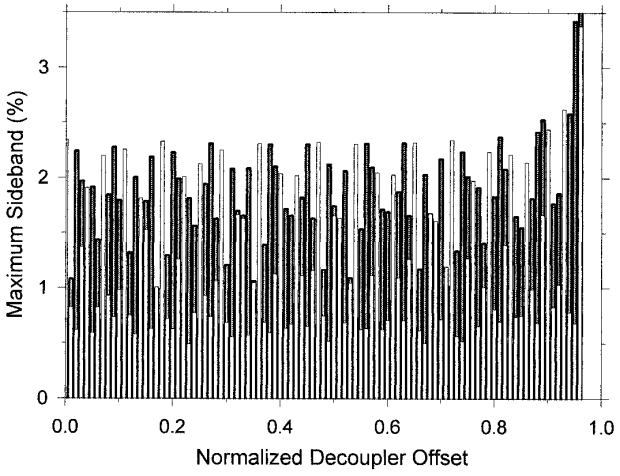

FIG. 1. The effect on sidebands of changing the initiating phase d in the phase cycle M4P5(d) of Eq. [1], evaluated for sech/tanh decoupling: unfilled, M4P5(150°); filled, M4P5(330°). Maximum sideband amplitude, expressed relative to the ideally decoupled central peak, is plotted as a function of decoupler offset, normalized to bwdth/2, the maximum of the adiabatic frequency sweep. The symmetric sideband distribution for negative resonance offset is not shown. Synthetic spectra (J_{CH} = 150 Hz) were generated according to the analysis given in (*15*). The relevant decoupling parameters, defined in Ref. (*1*), are RF_{max} = 6.7 kHz, the maximum B_1 amplitude; bwdth = 50 kHz, the total frequency range swept during the pulse; and T_p = 1.1 ms, the inversion pulse length. These values correspond to experimental parameters at the point labeled *b* in Fig. 3.

that produce their largest sidebands at different offsets and combine these two cycles, effectively averaging a large sideband at one offset with a smaller sideband obtained using the second value of d.

For a particular value of d, the above-stated goals can be achieved by constructing a second cycle with d incremented by 180°. Referring to Eq. [1], this amounts to adding 180° to every other element of the P5 cycle, starting with the second element. This procedure is different than standard iterative schemes (*13–15*) involving both cyclic permutation of elements and inversion of all RF phases in a sequence, but can be incorporated into these schemes. The utility of the resulting decoupling phase cycles, denoted by the value d as M4P5(d), is illustrated in Fig. 1 by overlaying step plots of maximum sideband as a function of decoupler offset for M4P5(150°) and M4P5(330°). Details are provided in the figure caption. When STUD is employed at low RF power, the largest sidebands within the decoupled bandwidth occur at frequencies of $1/(2T_p)$ or $1/(5T_p)$ relative to the central decoupled peak. Figure 1 shows that, at any particular offset, these sidebands can also be quite small compared to maximum sideband intensities over the full decoupled bandwidth. Since M4P5(330°) produces large sidebands at the offsets where M4P5(150°) sidebands are small, the net effect of either signal averaging or concatenating the two phase cycles is a significant reduction in maximum sideband amplitude over the bandwidth, as shown in Fig. 2.

Experimental verification of the method over a range of decoupling parameters is provided in Fig. 3, where maximum sideband amplitude over an effective decoupled bandwidth of 47 kHz is plotted as a function of reciprocal average power. Incrementing the value of d in steps of 30° from 0° to 330° in the concatenated phase cycle M4P5(d)–M4P5(d + 180°) produced no change in the maximum value of the sideband distribution over the decoupled bandwidth. Thus, we will refer to the improved cycle M4P5(d)–M4P5(d + 180°) more succintly as M4P5–M4P5′. No appreciable advantage was obtained by constructing cycles using more than two values of d. This new scheme should be generally applicable to other decoupling methods, and Fig. 3 also shows the improvements in performance that can be obtained when it is applied to WURST-40.

The lower limit to improvements in decoupling performance by this method occurs at high RF power, where maximum sideband amplitude is relatively insensitive to increases in RF power (*8*), as illustrated in Fig. 3. For STUD at the high-power limit, maximum sidebands occur at offsets of $\pm 1/T_p$ relative to the decoupled peak. These $1/T_p$ sidebands are established by the performance of the first inversion of

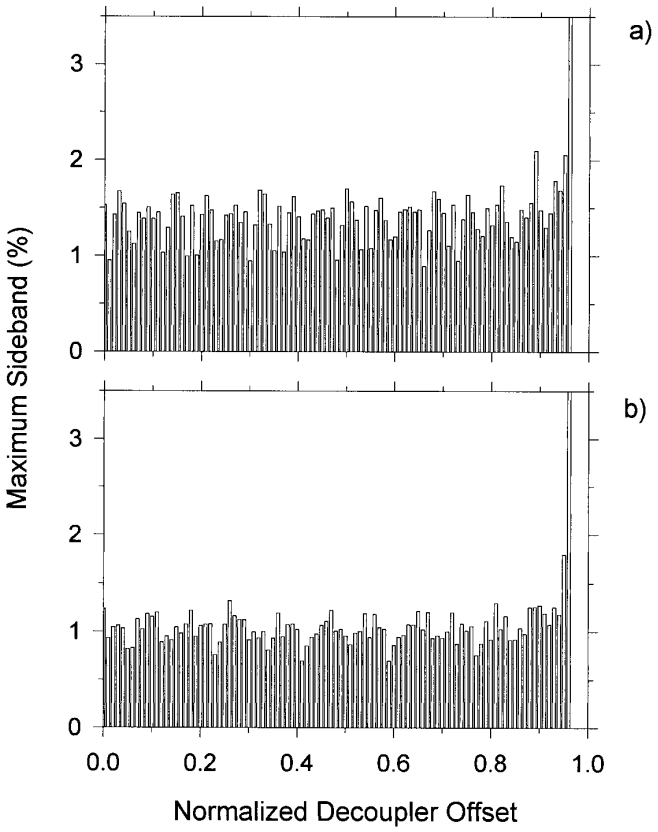

FIG. 2. As in Fig. 1, except the effect of sidebands is evaluated for (a) signal averaging separate M4P5(150°) and M4P5(330°) acquisitions and (b) a single acquisition using the concatenated cycle M4P5(150°)–M4P5(330°).

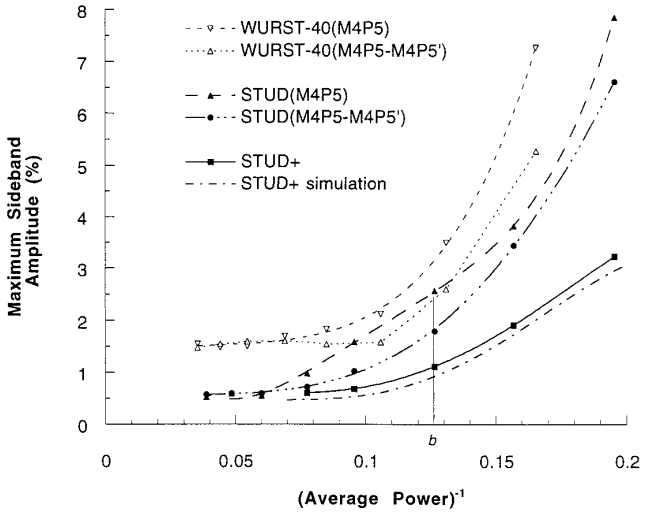

FIG. 3. Plots of maximum sideband amplitude versus reciprocal average power for various decoupling schemes. The units of (average power)$^{-1}$ are (kHz)$^{-2}$. Proton-detected ^{13}C-decoupled spectra (two transients) were generated by applying a heteronuclear spin-echo difference sequence (*21*) with the delays set to 3.33 ms to a sample of $^{13}CH_3I$ (J_{CH} = 150 Hz) in a 5 mm HCN triple-resonance PFG probe on a 500 MHz Varian INOVA spectrometer. Sideband amplitudes were measured as described in Ref. (*8*). To illustrate the trend in the data, curve fitting with fourth-order polynomials or a locally weighted method has been applied. In all cases, T_p = 1.1 ms, and for STUD, bwdth = 50 kHz, yielding an effective bandwidth of 47 kHz. To obtain the same effective bandwidth for WURST-40, bwdth = 61 kHz. In units of kHz^2, average power for STUD and WURST-40 are respective factors of 5.3 and 1.19 less than RF^2_{max}. The data for STUD can be compared to the calibration curves in (*8*) by multiplying the *x*-axis by 50.0/5.30. Since adiabatic decoupling schemes at a given T_p produce the same sideband levels at the same ratio of bwdth to average RF power (*8*), the results are valid for a wide range of bwdth values (at least 10–100 kHz). STUD+ results were obtained using sech/tanh decoupling implemented with the 112-phase cycle M4P5–M4P9–M4P5′–M4P9′. Equivalent performance is obtained by signal averaging acquisitions using M4P5–M4P9 and M4P5′–M4P9′. Theoretical results for STUD+ were derived from simulated decoupled spectra. The simulation was performed on resonance as a proxy for the maximum of the sideband distribution over the entire decoupled bandwidth and is therefore ~10% less than the experimental values (*22*). The simulation of Figs. 1 and 2 were obtained at an average power given by part *b* in the figure.

the decoupling sequence, before any compensation due to phase cycles can be implemented. An idealized model using instantaneous inversion pulses separated by delays of length T_p provides a good estimate of their intensity (*2*). They can also be shown by application of a straightforward vector model (*16*) to be a large fraction of $0.25\cos(1 - \pi J_r T_p/2)$, where J_r is the effective coupling constant during the single inversion, as in Fig. 10 of (*17*). For the high-power limit near a value of 0.05 (kHz)$^{-2}$ in the Fig. 3 results, $J_r \approx 0.93J$ and this simple analysis provides good agreement with experiment.

A seven-phase cycle derived according to the Tycko *et al.* algorithm (*6, 18*) is less efficient than the P5 cycle for sech/tanh decoupling, as determined previously (*1*). At any value of d, the corresponding M4P7 cycle produces larger sidebands than M4P5. Although the augmented sequence M4P7–M4P7′ significantly reduces sidebands compared to both M4P5 and M4P7 alone, it is still worse than M4P5–M4P5′. A nine-phase cycle we calculated using this algorithm (*18*) showed further comparative losses of decoupling efficiency, as did a separate seven-phase cycle designed to satisfy different criteria (*19*). However, Hwang *et al.* (*20*) have shown that M4P9 constructed from the nine-phase cycle (*19*)

$$[0°, 15°, 180°, 165°, 270°, 165°, 180°, 15°, 0°] \quad [2]$$

provides improved adiabatic decoupling performance compared to M4P5, and M4P5(150°)–M4P9(15°) was shown to provide a further reduction in sidebands. Although the nine-step cycle of Eq. [2] was not originally described in terms of a variable d value, it may be cast in this form as

$$[0°, d, 2d + 150°, 3d + 120°, 4d + 210°, 5d + 90°, 6d + 90°, 7d + 270, 8d + 240°] \quad [3]$$

providing leeway for constructing M4P5–M4P9(d)–M4P5′–M4P9(d + 180°). We will refer to this, using the previous shorthand notation, as M4P5–M4P9–M4P5′–M4P9′, since the maximum of the sideband distribution over the decoupled bandwidth is again relatively insensitive to the actual value of d.

Table 1 provides comparative results showing progressive reduction in maximum sideband amplitude as a result of applying our procedure to the efficient phase cycles dis-

TABLE 1

Results of Applying Various Phase Cycles Augmented with the New Algorithm to Sech/Tanh Dcoupling at an Average Power Given by Point *b* in Fig. 3 (bwdth = 50 kHz, T_p = 1.1 ms)

Phase cycle	No. of phases in cycle	Maximum sideband amplitude (%)
M4P5	20	2.56
M4P9	36	1.97
M4P5–M4P5′	40	1.67
P5P9	45	1.65
M4P5–M4P9	56	1.39
M4P5–M4P9–M4P5′	76	1.21
M4P5–P5P9–M4P5′	85	1.18
M4P5–M4P9–M4P5′–M4P9′	112	1.11

Note. Maximum sideband amplitude is measured over the effective decoupled bandwidth of 47 kHz. A prime on a phase cycle refers to shifting the initiating phase d (e.g., Eqs. [1], [3]) by 180° relative to the value used in the unprimed cycle. Performance equivalent to the 112-step cycle can be obtained by signal averaging separate acquisitions using M4P5–M4P9 and M4P5′–M4P9′.

cussed above. The table shows the best examples of concatenation as a function of cycle length from among more than 50 tested combinations of these cycles. For example, although the performance of the 72-step cycle M4P9–M4P9′ is significantly better than M4P9 alone, it is somewhat worse than the 56-step cycle listed in the table. The new nested cycle P5P9 provides the best result for any nonconcatenated cycle, but is not as useful as M4P5 or M4P9 in concatenated cycles because no advantage is gained in going to P5P9–P5P9′. Our new algorithm appears to work best when associated with an overlying MLEV-4 cycle. Triply nested cycles such as M4P5P9 show modest improvements over M4P5, but are not competitive with P5P9 or the subsequent concatenated cycles in Table 1. The order of the concatenation for the augmented cycles (i.e., $d \rightarrow d + 180°$) listed in Table 1 is important, as well. M4P5–M4P5′–M4P9–M4P9′ does not perform quite as well as M4P5–M4P9–M4P5′–M4P9′, and the same observation applies to M4P5–M4P9–M4P5′ and M4P5–P5P9–M4P5′.

From Table 1, the best method identified is the 112-phase cycle, M4P5–M4P9–M4P5′–M4P9′, which significantly reduces sideband amplitudes for sech/tanh decoupling, as shown in Fig. 3. Equivalent performance is obtained by signal averaging acquisitions using M4P5–M4P9 and M4P5′–M4P9′. We will refer to sech/tanh decoupling implemented with either form of this phase cycle as STUD+. Since the length of the 112-phase cycle will be a significant fraction of the signal acquisition time or T_2^* in routine one-dimensional experiments, diminishing returns can be expected for longer cycles. For many two-dimensional applications, the completion of this phase-cycle will exceed the acquisition time. Signal averaging using the two halves of the 112-step cycle would perhaps be preferable in such cases. For a 1 ms pulse length, the phase cycle would be 56 ms. Further work is required to determine whether the data in Table 1 are sufficient to determine the best phase cycle for acquisition times on the order of 100 ms or less.

The curve for STUD+ in Fig. 3 illustrates the improvements that can be expected relative to our recently published calibration curves for STUD (*8*) using M4P5. Until similar curves are available for STUD+, these calibration curves will suffice with the proviso that STUD+ provides a further reduction in sideband amplitude of up to a factor of three at low RF power. In addition, STUD+ provides effective bandwidths which are a few percent greater than those given by Fig. 7 of Ref. (*8*). We also include in Fig. 3 a simulation of maximum sideband amplitude as a function of average power for STUD+ to show that the experimental points are indeed connected by a smooth curve. Improvements in decoupling performance using STUD+ are significant, and these phase cycles appear to be generally applicable to other adiabatic decoupling techniques, as well.

In closing, we offer a brief synopsis for the applications spectroscopist of our experience in evaluating four other methods which might potentially improve adiabatic decoupling. (1) Asynchronous decoupling is commonly used in composite-pulse decoupling, but we find that for the most efficient adiabatic methods, failure to synchronize the decoupling pattern with signal acquisition actually increases sideband amplitudes. This phenomenon, confirmed by experiment, can be predicted from a vector analysis of the first inversion pulse (as briefly described above for the $1/T_p$ sidebands). (2) The utility of varying T_p between successive adiabatic pulses, while keeping the frequency-sweep parameter bwdth fixed, has been demonstrated by Hwang *et al.* (*23*). We have also varied T_p at fixed values of the product $T_p$bwdth, since the number of increments in the digitized decoupler waveform should be significantly greater than this product for good decoupling performance (*8, 17*). Experimentally, the two methods provide equivalent results. For k increments of T_p in the decoupling cycle, a given sideband at $1/(nT_p)$ is dispersed over a spectral range of $1/(nT_{p,1})$ to $1/(nT_{p,k})$ and resembles noise. However, the peak-to-peak amplitude of this ''sideband noise'' is not reduced significantly compared to the original sideband, which is especially problematic for sidebands which appear in dispersion mode. (3) Variation of T_p between successive transients, the ''accordian'' method of Starčuk *et al.* (2), is very effective in reducing the amplitudes of all sidebands. In general, a factor of five suppression of sidebands over eight transients can be achieved. (4) For STUD, the truncation of the sech waveform can be optimized, depending on the desired bwdth parameter, to obtain a 2–5% increase in effective bandwidth for the same average power.

Finally, we observe that adiabatic methods have been applied to ideal samples containing a single-coupling constant J_{CH} to demonstrate exceptional decoupled bandwidth while satisfying the constraints of low sideband intensity and sample heating. However, we recently identified a previously unrecognized problem that has significant implications for all adiabatic decoupling schemes (*22*). In cases where the pulse sequence prior to decoupling creates order in the S spins relative to the I spins, the subsequent coherent decoupling of the I spins may convert this order to additional sideband intensity. Optimal parameters of the preparation sequence can only be satisfied for a single J_{CH} in the sample. We have confirmed by theory and experiment (*24*) that departures from the optimal J_{CH} for the sequence can increase sideband intensity by an order of magnitude compared to sidebands produced under ideal conditions. Methods for eliminating this extra sideband intensity will be presented in more detail at a later date.

REFERENCES

1. M. R. Bendall, *J. Magn. Reson. A* **112,** 126 (1995).
2. Z. Starčuk, Jr., K. Bartušek, and Z. Starčuk, *J. Magn. Reson. A* **107,** 24 (1994).

3. M. S. Silver, R. J. Joseph, and D. I. Hoult, *J. Magn. Reson.* **59,** 347 (1984).
4. T. E. Skinner and M. R. Bendall, Abstracts of the 37th ENC, Asilomar, California, March 1996.
5. T. Fujiwara and K. Nagayama, *J. Magn. Reson.* **77,** 53 (1988).
6. R. Tycko and A. Pines, *Chem. Phys. Lett.* **111,** 462 (1984).
7. M. H. Levitt and R. Freeman, *J. Magn. Reson.* **43,** 502 (1981).
8. M. R. Bendall and T. E. Skinner, *J. Magn. Reson. A* **120,** 77 (1996).
9. Ē. Kupče and R. Freeman, *J. Magn. Reson. A* **117,** 246 (1995).
10. R. Fu and G. Bodenhausen, *J. Magn. Reson. A* **117,** 324 (1995).
11. Ē. Kupče and R. Freeman, *J. Magn. Reson. A* **115,** 273 (1995).
12. V. J. Basus, P. D. Ellis, H. D. W. Hill, and J. S. Waugh, *J. Magn. Reson.* **35,** 19 (1979).
13. M. H. Levitt and R. Freeman, *J. Magn. Reson.* **43,** 502 (1981).
14. M. H. Levitt, R. Freeman, and T. Frenkiel, *J. Magn. Reson.* **47,** 328 (1982).
15. J. S. Waugh, *J. Magn. Reson.* **49,** 517 (1982).
16. D. T. Pegg, M. R. Bendall, and D. M. Doddrell, *J. Magn. Reson.* **44,** 238 (1981).
17. M. R. Bendall, *J. Magn. Reson. A* **116,** 46 (1995).
18. R. Tycko, A. Pines, and J. Guckenheimer, *J. Chem. Phys.* **83,** 2775 (1985).
19. R. Tycko, A. Pines, and J. Guckenheimer, *Phys. Rev. Lett.* **56,** 1905 (1986).
20. T. L. Hwang, A. Tannus, M. Garwood, and P. C. M. Van Zijl, Abstracts of the 37th ENC, Asilomar, California, March 1996.
21. M. R. Bendall, D. T. Pegg, D. M. Doddrell, and J. Field, *J. Am. Chem. Soc.* **103,** 934 (1981).
22. T. E. Skinner and M. R. Bendall, *J. Magn. Reson. A* **123,** 111 (1996).
23. T.-L. Hwang, M. Garwood, A. Tannus, and P. C. M. van Zijl, *J. Magn. Reson. A* **121,** 221 (1996).
24. T. E. Skinner and M. R. Bendall, Abstracts of the 17th International Conference on Magnetic Resonance in Biological Systems, Keystone, Colorado, August 1996.